Endothelial NMDA receptors mediate activity-dependent brain hemodynamic responses in mice

Adam D. Hogan-Cann[a,b], Ping Lu[a,b], and Christopher M. Anderson[a,b,1]

[a]Department of Pharmacology and Therapeutics, Rady Faculty of Health Sciences, University of Manitoba, Winnipeg, MB, Canada R3E 0T6; and [b]Neuroscience Research Program, Kleysen Institute for Advanced Medicine, Health Sciences Centre, Winnipeg, MB, Canada R3E 0Z3

Dynamic coupling of blood supply with energy demand is a natural brain property that requires signaling between synapses and endothelial cells. Our previous work showed that cortical arteriole lumen diameter is regulated by *N*-methyl-D-aspartate receptors (NMDARs) expressed by brain endothelial cells. The purpose of this study was to determine whether endothelial NMDARs (eNMDARs) regulate functional hyperemia in vivo. In response to whisker stimulation, regional cerebral blood flow (rCBF) and hemodynamic responses were assessed in barrel cortex of awake wild-type or eNMDAR loss-of-function mice using two-photon microscopy. Hyperemic enhancement of rCBF and vasodilation throughout the vascular network was observed in wild-type mice. eNMDAR loss of function reduced hyperemic responses in rCBF and plasma flux in individual vessels. Discovery of an endothelial receptor that regulates brain hyperemia provides insight into how neuronal activity couples with endothelial cells.

NMDA receptor | hyperemia | neurovascular coupling | endothelium | two-photon microscopy

Functional hyperemia ensures that regional brain blood supply matches local metabolic demand and requires local vasodilation in active regions in addition to upstream conduction of vasomotor signals (1). Conducted responses are dependent on endothelial function (1, 2), but signaling between synapses and endothelial cells is poorly understood. *N*-methyl-D-aspartate receptors (NMDARs) are glutamate-gated, heterotetrameric ion channels composed of seven subunits (GluN1, GluN2A–D, GluN3A/B) (3). NMDARs have been studied extensively in neurons, but they are also expressed by endothelial cells (4). NMDAR activation dilates cerebral arteries ex vivo (5), and arteriolar vasodilation can be mitigated by selective endothelial NMDAR (eNMDAR) loss of function in cortical slices (4). The purpose of the current study was to determine whether eNMDARs regulate regional cerebral blood flow (rCBF) and hemodynamic responses in sensory hyperemia in vivo.

To study eNMDARs, floxed GluN1 mice (*grin1*fl/fl, JAX 005246) were crossed with mice expressing Cre-recombinase driven by Tie2 promoter elements (JAX 008863). *grin1*fl/fl · Cre+/− (Cre+) mice had eNMDAR loss of function, while *grin1*fl/fl · Cre−/− (Cre−) littermates were used as wild-type controls. Mice (30 to 40 d old) were craniotomized over the barrel cortex through a plastic plate implanted to permit head fixation during imaging. Before imaging by two-photon laser scanning microscopy (TPLSM), mice were injected with FITC-dextran to label plasma. Some mice received intracortical Fluo-4 (Ca^{2+}-sensitive dye) and SR101 (astrocyte label) for monitoring of neuronal activity. Head plates were secured in an air-supported mobile cage on the stage of a Bruker Ultima IV TPLSM instrument, allowing limb locomotion with fixed head.

Topological maps of vascular signals were created to a depth of ∼300 μm in layer II/III of the barrel cortex. Mice were subjected to contralateral whisker stimulation using trains of air puffs (10 Hz, 20-ms pulse, 10-s pulse train). Active areas were identified by surface artery dilations, and tracing flow identified penetrating arterioles (0th branch), precapillary arterioles (PCAs) (first order), and capillaries (third order or greater) (Fig. 1*A*). Line scans were used to study individual vessels. Scans parallel to the lumen were acquired sequentially and composited into space–time images that produced red blood cell (RBC) motion streaks along the lumen central axis. These were analyzed using a MATLAB toolbox, and RBC velocity was calculated using the Radon transform method (6). Transecting line scans were used to measure fluorescence intensity across the lumen diameter, which was calculated as the width spanning the 50% maximum points of the outer intensity projection peaks (6). Fig. 1*B* shows representative responses in penetrating arterioles. Plasma flux was derived mathematically from RBC velocity and lumen diameter ($F_{(t)} = \frac{\pi}{8} v_{(t)} d^2_{(t)}$) (7).

In Cre− control mice, all vessel subtypes dilated in response to whisker stimulation, with peak lumen diameter increases of 29 ± 8%, 23 ± 7%, and 28 ± 7% in penetrating arterioles, PCAs, and capillaries, respectively (Fig. 1*C*). Responses in PCAs were faster (50% maximum at 1.9 ± 0.3 s) than in penetrating arterioles (3.2 ± 0.3 s) and capillaries (3.1 ± 0.4 s) (Fig. 1*D*). Capillary plasma flux responses were significantly greater than PCA and penetrating arteriole responses during the 10-s stimulation (Fig. 1 *E* and *F*).

The mean, unstimulated lumen diameter of Cre− pial arteries was 21.4 ± 1.8 μm, while penetrating arterioles, PCAs, and capillaries had lumen diameters of 11.4 ± 0.5 μm, 8.7 ± 0.5 μm, and 4.5 ± 0.1 μm, respectively (Fig. 1*G*). Cre+ mice had ∼60% loss of endothelial GluN1 protein (4), but this did not influence baseline tone, RBC velocity, plasma flux (Fig. 1 *H* and *I*), or sensory-evoked neuronal Ca^{2+} responses (Fig. 1*J*). rCBF was assessed by laser Doppler flowmetry during whisker stimulation. In Cre− mice, rCBF peaked at 25 ± 2% over baseline (Fig. 2*A*). Cre expression mitigated the peak effect (10 ± 1%) and reduced the cumulative response during stimulation by 55 ± 4% (area under the curve). Increased lumen diameter and plasma flux were observed in penetrating arterioles, PCAs, and capillaries (Fig. 2 *B–D*). eNMDAR loss of function inhibited responses by more than 50% in each vessel subtype.

There are several reports that *grin1* levels are low in endothelial cells [e.g., refs. 8 and 9], raising the question of how a robust deletion phenotype could be produced. One possibility is that only certain endothelial cell phenotypes have significant *grin1*. This is supported by a recent finding that two of six brain endothelial cell subtypes identified had *grin1* at levels similar to astrocytes (10). It is also important to acknowledge that macrophages express Tie2 and consider the possible contribution of NMDARs in these cells. This is unlikely because perivascular
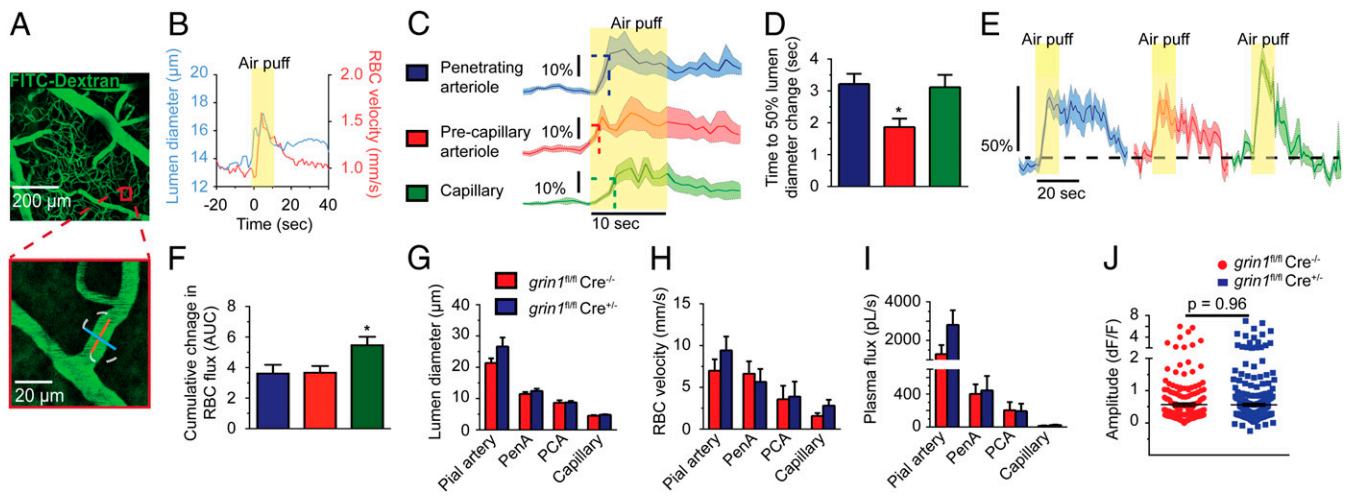
Fig. 1. Sensory-evoked hemodynamic responses in awake mice. Head-fixed mice were imaged in an air-supported mobile cage. (*A*) Cortical vascular network mapping identified distinct vessel subtypes. Line scans allowed calculation of RBC velocity, lumen diameter (*B*), and plasma flux following whisker stimulation. (*C–F*) Time to vasodilatory onset and cumulative plasma flux in different vessel subtypes. *$P < 0.05$ compared with other groups using ANOVA and Tukey's multiple comparison test. (*G–I*) Baseline lumen diameter, RBC velocity, and plasma flux throughout the vascular network. (*J*) Sensory-evoked neuronal Ca^{2+} responses in barrel cortex, in *grin1*$^{fl/fl}$ · Cre$^{-/-}$ and *grin1*$^{fl/fl}$ · Cre$^{+/-}$ mice. AUC, area under the curve; PenA, penetrating arteriole.

brain macrophages are located in the Virchow–Robin space, between the glia limitans and vascular basement membranes in larger cerebral vessels. We observed hemodynamic effects in smaller vessels, suggesting that macrophages were not required. In addition, studies in Tie2-GFP rodents revealed that Tie2$^+$ macrophages were not associated with brain blood vessels (11)

and that Tie2 was absent from the choroid plexus, which is a rich source of resident brain macrophages (12).

We previously showed that GluN1 is expressed at basolateral endothelial membranes and that cortical vasodilation is mitigated by eNMDAR loss of function (4). The current results show that eNMDARs regulate activity-dependent CBF responses,
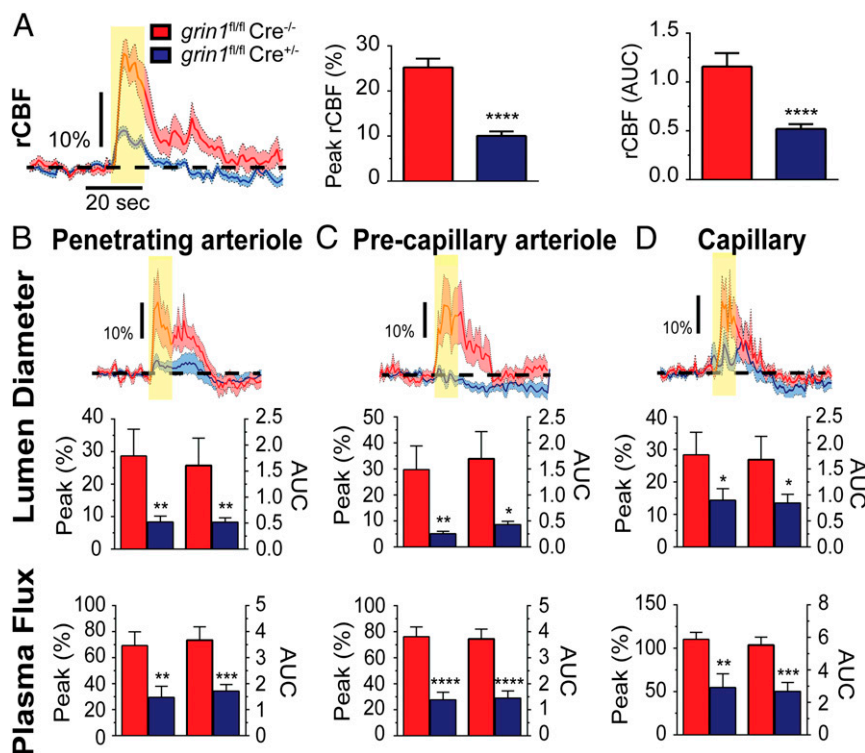
Fig. 2. Endothelial GluN1 silencing impairs functional hyperemia in awake mice. (*A*) Relative changes in barrel cortical blood flow following whisker stimulation, assessed by laser Doppler flowmetry. (*B–D*) Evaluation of eNMDAR loss of function (*grin1*$^{fl/fl}$ · Cre$^{+/-}$) on peak (left axis and left group of bars) and cumulative [right axis and right group of bars; time-course area under the curve (AUC)] lumen diameter and plasma flux responses in penetrating arterioles, precapillary arterioles, and capillaries (control: *grin1*$^{fl/fl}$ · Cre$^{-/-}$). *$P < 0.05$, **$P < 0.01$, ***$P < 0.001$, ****$P < 0.0001$ compared with *grin1*$^{fl/fl}$ · Cre$^{-/-}$ groups using two-tailed *t* tests.

in vivo. There is growing recognition that the cerebral endothelium is necessary for hyperemic CBF regulation (1), and that diseases of endothelial dysfunction contribute to cognitive decline (13). Our discovery of an endothelial receptor that regulates hyperemic hemodynamics provides insight into how neuronal activity couples with the cerebral endothelium and attributes a critical regulatory process to a well-known receptor at a unique cellular locus. Animals were used in accordance with the guidelines of the Canadian Council on Animal Care. The University of Manitoba Protocol Management and Review Committee has attested to this compliance by approving our animal use protocol (15-012).

1. Chen BR, Kozberg MG, Bouchard MB, Shaik MA, Hillman EM (2014) A critical role for the vascular endothelium in functional neurovascular coupling in the brain. *J Am Heart Assoc* 3:e000787.
2. Longden TA, et al. (2017) Capillary K$^+$-sensing initiates retrograde hyperpolarization to increase local cerebral blood flow. *Nat Neurosci* 20:717–726.
3. Traynelis SF, et al. (2010) Glutamate receptor ion channels: Structure, regulation, and function. *Pharmacol Rev* 62:405–496.
4. Lu L, et al. (2019) Astrocytes drive cortical vasodilatory signaling by activating endothelial NMDA receptors. *J Cereb Blood Flow Metab* 39:481–496.
5. LeMaistre JL, et al. (2012) Coactivation of NMDA receptors by glutamate and D-serine induces dilation of isolated middle cerebral arteries. *J Cereb Blood Flow Metab* 32: 537–547.
6. Barrett MJP, Ferrari KD, Stobart JL, Holub M, Weber B (2018) CHIPS: An extensible toolbox for cellular and hemodynamic two-photon image analysis. *Neuroinformatics* 16:145–147.
7. Shih AY, et al. (2009) Active dilation of penetrating arterioles restores red blood cell flux to penumbral neocortex after focal stroke. *J Cereb Blood Flow Metab* 29: 738–751.
8. Zhang Y, et al. (2014) An RNA-sequencing transcriptome and splicing database of glia, neurons, and vascular cells of the cerebral cortex. *J Neurosci* 34:11929–11947.
9. Zeisel A, et al. (2018) Molecular architecture of the mouse nervous system. *Cell* 174: 999–1014.e22.
10. Vanlandewijck M, et al. (2018) A molecular atlas of cell types and zonation in the brain vasculature. *Nature* 554:475–480.
11. Sabbagh MF, et al. (2018) Transcriptional and epigenomic landscapes of CNS and non-CNS vascular endothelial cells. *eLife* 7:e36187.
12. Ohtsuki S, Kamiya N, Hori S, Terasaki T (2005) Vascular endothelium-selective gene induction by Tie2 promoter/enhancer in the brain and retina of a transgenic rat. *Pharm Res* 22:852–857.
13. Iadecola C (2017) The neurovascular unit coming of age: A journey through neurovascular coupling in health and disease. *Neuron* 96:17–42.